Royal Netherlands Institute for Sea Research

de Nooijer, L. J., Hathorne, E. C., Reichart, G. J., Langer, G., & Bijma, J. (2014). Variability in calcitic Mg/Ca and Sr/Ca ratios in clones of the benthic foraminifer *Ammonia tepida*. Marine Micropaleontology, 107, 32-43.

Published version: http://dx.doi.org/10.1016/j.marmicro.2014.02.002

Link NIOZ Repository: www.vliz.be/nl/imis?module=ref&refid=239927

[Article begins on next page]

Variability in calcitic Mg/Ca and Sr/Ca ratios in clones of the benthic foraminifer *Ammonia tepida*

L.J. de Nooijer[a]*, E.C. Hathorne[b], G.J. Reichart[a,c], G. Langer[d], J. Bijma[e]

[a] Royal Netherlands Institute for Sea Research, Landsdiep 4, 1797 SZ, 't Horntje, The Netherlands, ldenooijer@nioz.nl

[b] GEOMAR Helmholz Centre for Ocean Research Kiel, Wischhofstrasse 1-3, 24148 Kiel, Germany

[c] Utrecht University, Department of Geochemistry, Budapestlaan 4, 3584 CD, Utrecht, the Netherlands

[d] Cambridge University, Department of Earth Sciences, Downing Street, Cambridge CB2 3EQ, United Kingdom

[e] Alfred Wegener Institute, Am Handelshafen 12, 27570 Bremerhaven, Germany

*Corresponding author: ldenooijer@nioz.nl, +49-(0)222-369380

Abstract

Biological activity introduces variability in element incorporation during calcification and thereby decreases the precision and accuracy when using foraminifera as geochemical proxies in paleoceanography. This so-called 'vital effect' consists of organismal and environmental components. Whereas organismal effects include uptake of ions from seawater and subsequent processing upon calcification, genetic and ontogeny, environmental effects include migration- and seasonality-induced differences. Triggering asexual reproduction and culturing juveniles of the benthic foraminifer *Ammonia tepida* under constant, controlled conditions allows environmental and genetic variability to be removed and the effect of cell-physiological controls on element incorporation to be quantified. Three groups of clones were cultured under constant conditions while determining their growth rates, size-normalized weights and single-chamber Mg/Ca and Sr/Ca using laser ablation-inductively coupled plasma-mass spectrometry (LA-ICP-MS). Results show no detectable ontogenetic control on the incorporation of these elements in the species studied here. Despite constant culturing conditions, Mg/Ca varies by a factor of ~4 within an individual foraminifer while intra-individual Sr/Ca varies by only a factor of 1.6. Differences between clone groups were similar to the intra-clone group variability in element composition, suggesting that any genetic differences between the clone-groups studied here do not affect trace element partitioning. Instead, variability in Mg/Ca appears to be inherent to the process of bio-calcification itself. The variability in Mg/Ca between chambers shows that measurements of at least 6 different chambers are required to determine the mean Mg/Ca value for a cultured foraminiferal test with a precision of ≤10%.

Key words: Benthic foraminifera, Mg/Ca, Sr/Ca, Laser ablation ICP-MS, Inter-individual variability, Intra-individual variability

1. Introduction

Incorporation of various trace elements into foraminiferal calcite is affected by environmental parameters and therefore, calcitic element/calcium ratios are widely used to reconstruct marine paleoenvironments. For example, foraminiferal Mg/Ca ratios have been shown to be primarily correlated with seawater temperature (e.g. Nürnberg et al., 1996) and are used in combination with test calcite $\delta^{18}O$ to reconstruct paleo-seawater $\delta^{18}O$ (e.g. Elderfield and Ganssen, 2000; Lear et al., 2000), and estimate salinity. Elevated Mg-incorporation into calcite at higher temperatures has also been reported from inorganic precipitation experiments (Mucci, 1987; Oomori et al., 1987). However, the relative increase in Mg/Ca with temperature for foraminifera is greater than reported for inorganically precipitated calcites (~10% per ºC compared to <5% per ºC, respectively), suggesting that foraminiferal Mg/Ca is largely controlled by biological activity (Rosenthal et al., 1997; Erez, 2003; De Nooijer et al., 2009a; 2009b; Wit et al., 2012). The cellular control on Mg-incorporation is also reflected by the low Mg/Ca ratios of most foraminiferal species compared to calcite precipitated from seawater (Blackmon and Todd, 1959; Bentov and Erez, 2006). Furthermore, Mg/Ca varies also within single individual foraminifer tests (e.g. Hathorne et al., 2003; Toyofuku and Kitazato, 2005) and through chamber walls (e.g. Eggins et al., 2004; Sadekov et al., 2005; Kunioka et al., 2006; Hathorne et al., 2009).

The origin of intra-individual and intra-chamber wall Mg/Ca heterogeneity in benthic and planktonic species remains enigmatic. Previous work suggested that ontogenetic (i.e. life-stage related) changes can be responsible for intra- and inter-test Mg/Ca variability in benthic foraminifera (Hintz et al., 2006; Filipsson et al., 2010, Raitzsch et al., 2011a; Diz et al., 2012). Ontogeny can affect trace element partitioning through changes in physiology, growth rate or changes in surface area-volume ratios. Migration into different environments with age and

life-stage may be responsible for part of the observed effects, but this is an environmental control rather than ontogeny as such. Additionally, inter-individual variability in Mg/Ca may potentially be caused by genetic differences between individuals of the same species (Numberger et al., 2009).

Foraminiferal Sr/Ca is positively correlated with temperature in a number of species (Rathburn and De Deckker, 1997; Reichart et al., 2003; Mortyn et al., 2005; Rosenthal et al., 2006; Kisakürek et al., 2011), salinity (Dissard et al., 2010a; Kisakürek et al., 2011) and seawater Sr/Ca (Delaney et al., 1985; Elderfield et al., 2000; Raitzsch et al., 2010). Reported inter- and intra-individual variability in Sr/Ca is smaller than observed for Mg/Ca (e.g. Dueñas-Bohórquez et al., 2009; 2011a). The partition coefficient for Sr incorporation is closer to that found in inorganic precipitation experiments (e.g. Lorens, 1981; Tesoriero and Pankow, 1996; Delaney et al., 1985; Dissard et al., 2010a) when compared to Mg incorporation (e.g. Mucci, 1987; Delaney et al., 1985; Nürnberg et al., 1996). This difference suggests that incorporation of Sr is not under the same biological control as Mg, and that the absence of this control causes the relatively homogenous inter-species, intra-species and intra-individual incorporation.

The elemental and isotopic composition of individual tests is increasingly used for estimating past inter and intra-annual change, such as seasonality (Wit et al., 2010; Ganssen et al., 2011, Haarmann et al., 2011; Khider et al., 2011). The accuracy of such reconstructions, however, critically relies on the ability to distinguish vital effect-related variability from that caused by the environment. Here, we cultured genetically identical individuals of the shallow-water benthic foraminifer *Ammonia tepida* under constant environmental conditions, monitoring ontogenetic variability to constrain the intrinsic natural amplitude of Mg/Ca and Sr/Ca variability between and within individuals. *Ammonia* spp. produce calcite with a very low Mg/Ca (~1 mmol/mol), indicating a strong biological control on Mg-incorporation. This

implies that changes in this biological control also are expected to have a relatively large impact compared to other foraminiferal species. Hence by studying this species we are able to capture the maximum impact related to variability in the vital effect. The intrinsic natural variability of Mg/Ca and Sr/Ca ratios ultimately determines how well we will be able to constrain past seasonal temperature variability and provides constraints for the biologically induced noise in reconstructions.

2. Methods

2.1 Culturing and reproduction

Surface sediments were collected from the muddy intertidal flats near Dorum, Northwestern Germany (53º44'16 N, 8º30'53 E) in autumn 2008. Average Wadden Sea water temperature in October is ~13 °C, with an average diurnal variability of ~1 °C (Van Aken, 2008). Upon return to the laboratory, sediment was sieved over 1-mm screens to remove the largest macrofauna and stored at 10°C. Prior to incubation, small amounts of sediment were sieved over a 250 µm-screen to retrieve large living individuals of *Ammonia tepida*. Individuals with brightly yellow colored cytoplasm were regarded as living and isolated for incubation. Four groups of 25 individuals were placed in Petri dishes with approximately 50 ml of 0.2 µm-filtered North Sea water (salinity 32), fed with living *Dunaliella salina* by adding 300 µL of a densely concentrated algae culture (approximately $3x10^6$ cells/ mL) and brought instantaneously to 25 ± 0.5°C at which they were kept until reproduction.

Adult, megalospheric foraminifera underwent asexual reproduction at regular intervals (Figure 1), resulting in the production of 50-300 megalospheric, one-chambered juveniles emerging from the same adult test. The size of these one-chambered juveniles ranges from approximately 20 to 30 µm, suggesting that they are gamonts (as opposed to schizonts; Goldstein and Moodley, 1993; Stouff et al., 1999). Theses juveniles were isolated from their

parent test and kept together in a new Petri dish. All juveniles resulting from one asexual reproductive event (i.e. having the same individual parent) will be referred to as a 'clone group'. Since the parents of these clone groups come from the same sample location, it may be that the different clone groups are genetically closely related. Juveniles from three of these clone groups were kept in three separate Petri dishes and fed once a week. The water in these dishes was changed every two days. At the beginning and end of the incubations, salinity (32.2 ± 0.2) and pH (8.14 ± 0.05, NBS scale) were measured using a 330i WTW conductivity meter and WTW pH3000 with Schott BlueLine electrodes, respectively. Culture media subsampled for DIC (2193 ± 29 µM) was filtered over 0.2 µm filters and measured photometrically using a XY-2 sampler (Bran + Lübbe GmbH, Norderstedt, Germany). Subsamples were also analyzed for [Mg^{2+}] (49 ± 2 mmol/kg), [Ca^{2+}] (9.5 ± 0.05 mmol/kg) and [Sr^{2+}] (90 ± 0.8 µmol/kg) using ICP-OES. Uncertainties for these concentrations (± 1 standard deviation) represent differences between replicate measurements (n=4).

For a different set of three clone groups, the size of individuals was determined by regular observation under an inverted microscope and counting the number of chambers of each individual. After 3 weeks of incubation in the same artificial seawater in which the other three clone groups were kept, specimens were taken out and cleaned. Specimens both from the culturing experiment and from the incubation to determine growth rates were placed in buffered NaOCl (15%) for 24 hours to remove organic material. Individuals were then rinsed several times with double deionized water and dried at 60°C for several hours. Multiple individuals from one group with the same number of chambers (ranging from 6-16 chambers) were weighed on a UMX2 microbalance (Mettler Toledo, precision ± 0.1 µg) to determine "chamber-normalized" weights. Other studies have reported size-normalized weights based on the diameter (e.g. De Moel et al., 2009; Beer et al., 2010) of analyzed individuals, but to

150 facilitate comparison of growth with the LA-ICP-MS data (see section 3.3) size-normalized
151 weights and growth rates are expressed per total number of chambers.
152
153 Figure 1: Asexual reproduction in *Ammonia tepida*. The empty test of the adult (i.e. 'parent')
154 individual is surrounded by approximately 200 juveniles that have emerged from the aperture.
155 The single-chambered juveniles form a relatively large and dense pseudopodial network that
156 they use to move away from the parent in the following hours. The dark masses are remains
157 of the food cyst that surrounded the adult foraminifer before reproduction. Scale bar = 100µm.
158
159 Since a large number of geno- and morphotypes have been reported for *Ammonia* (e.g.
160 Holzmann and Pawlowski, 1997; 2000; Debenay et al., 1998; Hayward et al., 2004), culturing
161 individuals from one clone group overcomes the potential imprint of genetic variability on
162 calcite chemistry. This is particularly important since the genus of *Ammonia* is widely studied,
163 but named differently by different researchers. At our sampling location, 'Ammonia molecular
164 type T6' is the dominant ~~morpho~~type ~~(Hayward et al., 2004)~~, and will be referred to here as *A.*
165 *tepida*.
166
167 *2.2 LA-ICP-MS*
168 Three laser ablation systems coupled to inductively coupled plasma-mass spectrometers (LA-
169 ICP-MS) were used during the course of this study (Table 1). The majority of analyses were
170 conducted at the University of Bremen using a solid state 193 nm laser ablation system (New
171 Wave Research) coupled to an Element2 (Thermo Scientific) sector field ICP-MS. The ICP-
172 MS was run in low resolution mode without the shield torch and the measurement routine
173 took 1.4 s to cycle through the masses. Masses monitored were ^{11}B, ^{25}Mg, ^{27}Al, ^{43}Ca, ^{55}Mn,
174 ^{66}Zn, ^{88}Sr, ^{137}Ba and ^{238}U. All ablations were conducted in He and lasted up to 60 seconds

175 before the shell wall was penetrated using laser spots of 35 or 75 μm in diameter, a repetition
176 rate of 5 Hz, and a laser power density of ~0.35 GW/cm^2. A NIST SRM 610 glass was used
177 for calibration and ablated with a laser power density of ~1 GW/cm^2 between every 5 or 10
178 sample analyses. Calibration of element/calcium ratios in calcium carbonate samples using a
179 NIST glass standard has been demonstrated to be accurate for many elements when using a
180 193 nm laser (Hathorne et al., 2008). The precision of the technique is ~4% (1σ) for Mg/Ca
181 and Sr/Ca based on many spot analyses of powder pellets of carbonate reference materials
182 (e.g. Raitzsch et al., 2011a).
183
184 Table 1: Settings and details of the different laser systems employed in this study.
185
186 Time resolved signals were selected for integration, background subtracted, internally
187 standardized to ^{43}Ca, and calibrated with the signals from the NIST SRM610 using the
188 GeoPro software (Cetac). Despite the removal of organics with NaOCl it was clear from the
189 time resolved laser signals that some cytoplasm, with elevated Mg and Zn, remained on the
190 outside and inside of a few chambers. Zinc is known to be concentrated by phytoplankton (Ho
191 et al., 2003), adding to the intracellular concentrations in the foraminifera when taken up as
192 food. Parts of analyses, towards the outside or inside of the test wall, with elevated Mg and Zn
193 were omitted from the integration (Figure 2C). In some cases where the test wall was thin, the
194 ablation was very short and the Mg and Zn levels remained high throughout. Such analyses
195 were discarded and not considered further. Screening of time resolved signals for surface
196 contamination is a standard practice to ensure that only contaminant-free data are considered
197 (e.g. Reichart et al., 2003; Sadekov et al., 2008; Hathorne et al., 2009).
198 As a solid state laser system is not optimized for depth profiling, a number of cultured tests
199 were also analyzed using a 193 nm ArF Excimer laser at Utrecht University (GeoLas 200Q)

and at the GEOMAR in Kiel (New Wave) to acquire depth-profiles of the element/Ca ratios through the shell walls (Table 1). The analyses at Utrecht also used an Element2 (Thermo Scientific) sector field ICP-MS. The laser at the GEOMAR is equipped with a large format cell with a low volume (~1 cm^3) ablation chamber that is optimal for such depth profiling analyses and employed an Agilent 7500cs ICP-MS. Calibration and standardization also used the NIST SRM 610 glass (values from Jochum et al., 2011) that was ablated using a higher laser fluence of ~4 J/cm^2. The raw time resolved counts were blank subtracted, internally standardized to ^{43}Ca and calibrated using standard spreadsheet software to obtain depth profiles for Sr/Ca and Mg/Ca ratios. Data were further processed with a 2σ outlier rejection to remove the odd flier and smoothed with a 3 points running average to obtain the depth profile (data from Bremen were not treated in this way as only average values for each laser spot were obtained). Analyses of a powder pellet of the JCp-1 carbonate reference material agree with the recommended values in the literature (Okai et al., 2002; 2004) and indicate a within depth profile precision of <20% (1σ). A similar result was obtained by depth profiling through an Iceland spar calcite used in the Utrecht laboratory.

Figure 2: Example of two individuals (A and B) after LA-ICP-MS. P=proloculus, F=final chamber. Scale bar = 100μm. C: example of a laser ablation profile with high Mg/Ca and Zn/Ca indicative of residual cytoplasm on both sides of the chamber wall.

Using the obtained foraminiferal Mg/Ca and Sr/Ca and those of seawater, apparent partition coefficients for these elements in the calcite of *Ammonia tepida* are calculated as follows:

$$D_{Element} = (Element/Ca)_{calcite}/(Element/Ca)_{medium}$$

225 **3. Results**

226

227 *3.1 Reproduction, growth rates and size-normalized weights*

228 The number of juveniles that result from one reproductive event varied between the clone
229 groups (Table 2). The maximum size (diameter) that was reached at the end of the culturing
230 period also varied, resulting in analyses being performed on individuals with a range of sizes.

231

232 Table 2: Reproduction, growth and amount of calcite available for chemical analyses. Dextral
233 coiling is clockwise addition of chambers on the spiral side: sinistral is anti-clockwise. 'n.d.'=
234 not determined.

235

236 Growth rates (expressed here as number of chambers added per day) varied between clone
237 groups, although the general pattern was similar between groups: as size increases, growth
238 (chamber addition) rates decrease. Chamber-normalized weights as determined after the
239 culturing experiments show that the amount of calcite precipitated per chamber increases with
240 size (Figure 3).

241

242 Figure 3: Growth rates (A, ± 1 standard deviation) for each of the three clone groups and
243 chamber-normalized weights (B) of cultured *A. tepida*. The weight of tests increases
244 exponentially with every chamber being added (R^2=0.934; compared to 0.888 for a linear fit)
245 and is described by: $w=0.138e^{0.225n}$, where w is the $CaCO_3$ weight of an individual test in µg
246 and n is the chamber number (1= proloculus).

247

248 *3.2 Test wall variability in Sr/Ca and Mg/Ca*

Ablation profiles obtained with the excimer laser systems at Utrecht and Kiel from different chambers of one individual show that inner chambers are progressively thicker because of bilamellar calcification. This is visible from the length of profiles as they become longer (before returning to background values) when ablating chambers that were formed at earlier lifestages of the foraminifers.

Within the obtained profiles, Sr/Ca varies between 1.0 and 2.5 mmol/mol (Figure 4A). On average, Sr/Ca of these profiles was 1.42 mmol/mol and the average standard deviation of a profile is 0.32 mmol/mol. Mg/Ca in profiles from the same measurments var~~y~~ between 2 and 14 mmol/mol within ~~one~~ chamber wall (Figure 4B). Average Mg/Ca in these profiles ~~vary~~ between 1.8 and 6.1 mmol/mol, with an average standard deviation of 1.2 mmol/mol for one profile. The obtained average Mg/Ca for these profiles match the range in Mg/Ca from the larger dataset (section 3.3; Figure 5B). Variability in average Mg/Ca between laser ablation spots is caused by the occasional occurrence of calcite with high Mg/Ca (Figure 4B, chamber F-6; Figure 4C, chamber F-5). These parts ~~of~~ elevated Mg/Ca, however, are not present in all chambers, ~~nor~~ their position or number per chamber wall the same for different chambers within ~~any~~ individual.

Figure 4: Sr/Ca and Mg/Ca ablation profiles from cultured *Ammonia tepida*. ~~A~~: Sr/Ca of one chamber obtained at Utrecht University (in black) and one obtained at GEOMAR (in blue), B: Mg/Ca of three different chambers obtained at Utrecht University, C: Mg/Ca of three different chambers obtained at GEOMAR.

Average Sr/Ca and Mg/Ca and the variability in these profiles (Figure 4) are similar for the different laser systems employed. This not only facilitates direct comparison between the data

obtained by us, but also demonstrates the reproducibility of the Sr/Ca and Mg/Ca ratios despite differences in ablation cell design.

3.3 Interchamber and size-related variability in Sr/Ca and Mg/Ca

When combining the average values from the ablation profiles with the 173 spot analyses obtained at the University of Bremen, Sr/Ca of all ablation profiles range between 1.2 and 2.0 mmol/mol (Figure 5A), with an average of 1.6 mmol/mol (± 0.13 mmol/mol standard deviation). No trend for Sr/Ca and chamber number is detectable (data of all clone groups combined, as well as for separate groups: regression analysis, $R^2 < 0.001$). In 15 cases, 2 measurements were performed on a single chamber (Figure 2A). The average difference between these pairs of measurements is 0.084 mmol/mol (± 0.072 standard deviation) and smaller than the overall variability in Sr/Ca (Figure 5A).

Average Mg/Ca of single laser ablation spots range between 1 and 8 mmol/mol (Figure 5B), with an average ratio of 3.6 mmol/mol (± 1.2 standard deviation) and no ontogenetic trend (regression analysis, $R^2 < 0.001$). Nor was there a significant difference in Sr/Ca or Mg/Ca between coiling directions. For the 15 pairs of measurements on the same chamber, the average difference in Mg/Ca from these spots is 0.48 mmol/mol (± 0.64 standard deviation), which equals 16% of the average Mg/Ca. This average difference is comparable to the average difference between two laser ablation measurements randomly taken from the complete dataset (see end of this section).

Figure 5: Average Sr/Ca (panel A), Mg/Ca (panel B) and partition coefficients (D_{Sr} and D_{Mg}) from single-chamber analyses of 30 individuals of cultured *A. tepida* as a function of the position within the foraminifer. Every point represents one laser ablation spot. On the left side, analyses of the final (F) chamber are plotted, while measurements towards the right side

represent Sr/Ca and Mg/Ca from older chambers. Black, grey and white symbols represent the three different clone groups. Larger circles represent average Sr/Ca and Mg/Ca for each chamber position. The dotted line and surrounding grey box represent the average ± 1 standard error of the mean. The lighter grey box represents ± 1 standard deviation. Number of laser ablation spots per chamber position is indicated in at the upper side of panel B.

The variability (standard deviation) between single-chamber Mg/Ca (± 33% of the average; Figure 5B) is larger than for Sr/Ca (± 8% of the average; Figure 5A). The large number of measurements results in a small standard error of the mean (<1% and ~5% for Sr/Ca and Mg/Ca, respectively; Figures 5A and B).

When comparing chambers counting from the proloculus onward (i.e. 'backwards' compared to the order as is used in Figures 5), there is no trend in Sr/Ca (nor in Mg/Ca) with chamber number. The layering caused by so-called bilamellar calcification in Rotallid species (Reiss, 1957; Erez, 2003) means that we prefer to compare chambers that have ~~an equal number~~ of lamellae (thus comparing all F chambers, F-1, etc; Figures 5A and B).

Not all individuals had the same number of chambers at the end of the experiment, which might mask (subtle) ontogenetic trends in element/Ca ratios. Therefore we also tested for changes in Sr/Ca and Mg/Ca with chamber number within individuals. For the 22 individuals that were ablated 3 or more times, no significant intra-individual trend was observed in Sr/Ca or Mg/Ca (Student-T test using residual sum of squares from a linear regression, $p<0.05$). Since some individuals have the same final number of chambers, these tests were repeated on results combined for individuals with 18, 17, 16, 15, 8 and 7 chambers. None of the resulting regression analyses and T-tests indicated a significant increase or decrease of Sr/Ca or Mg/Ca with chamber number. Finally, we compared all F-chambers measured (n=16) and conducted

a regression analysis for Sr/Ca and Mg/Ca as a function of final number of chambers. This too revealed no significant trend with chamber number.

To evaluate the relation between the number of observations (i.e. laser ablation spots) and the representativeness of the resulting average Mg/Ca of all measurements, a Monte Carlo Permutation test was executed. From all 207 laser ablation-determined Mg/Ca ratios, a randomly selected ratio was taken to calculate the deviation from the average Mg/Ca (=3.6 mmol/mol). This was repeated 50 times to calculate the average deviation from the data set's mean Mg/Ca (based on 207 laser ablation measurements). This value approximates the uncertainty in Mg/Ca when using only one laser spot to determine the average Mg/Ca in a dataset like ours. This procedure was repeated by taking 50 sets of two randomly selected Mg/Ca to calculate the average deviation from the dataset's mean Mg/Ca, then taking 50 sets of three randomly selected Mg/Ca, etc (Figure 6). The relationship between number of laser ablation spots and the deviation from the dataset's average resembles $1/\sqrt{n}$.

Figure 6: relation between number of laser ablation spots and deviation from the set average Mg/Ca (n=50, see text for explanation) from the average Mg/Ca of the complete dataset (=3.6 mmol/mol). With ~6 laser ablation measurements on different chambers (or positions on the test) the deviation is approximately 10% of the average of the dataset, with ~20 measurements, the estimated Mg/Ca is within 5% of the average of the complete dataset.

3.4 Interindividual variability in Sr/Ca and Mg/Ca

Combining results from laser ablation spots on the same individual (on average 7.7 spots) provides an estimate of variability in Sr/Ca and Mg/Ca between the 25 analyzed individuals

346 (Figure 7). The three individuals with less than 3 laser ablation spots/ individual are not
347 discussed further in this section.
348
349 Figure 7: A: Variability of single individual Sr/Ca in cultured *A. tepida*. Results from all laser
350 spots (Figure 5A) are combined to display the inter-individual variability in Sr/Ca (average
351 per individual ± 1 standard deviation). These data have been ranked according to their Sr/Ca
352 ratio ~~for clarity but~~ note that the ranking for inter-individual Mg/Ca is different. B: Variability
353 of Mg/Ca in cultured individuals. Results from single-chamber measurements (Figure 5B) are
354 combined to display the inter-individual variability in Mg/Ca (average per individual ± 1
355 standard deviation). For both panels, dotted horizontal line is the average element/Ca of all
356 individuals and accompanying dark grey box represents 1 standard deviation.
357
358 To compare the Sr/Ca and Mg/Ca between individuals, a one-way ANOVA test was
359 performed for every possible pair of individuals, 231 in total. Of all these pairs, the Mg/Ca of
360 80 pairs of individuals (35%) were significantly different ($p<0.05$). Of these 80 pairs, only
361 four indiviudals are involved in 51 pairs. This means that, with the exception of these four
362 individuals (two at the far left and two at the far right side in figure 7A), the average Mg/Ca
363 of 87% of all possible combinations of two individuals are not significantly different from
364 each other. Inter-individual differences for Sr/Ca are similar with 67 out of 231 pairs (29%)
365 that are being significantly different. Of these 67 pairs, three individuals (one at the left side
366 and two at the far right side in figure 7B) are involved in 31 significantly different average
367 individual's Sr/Ca. This means that excluding these three individuals, average Sr/Ca of 84%
368 of all possilbe combinations of two individuals are not significantly different from each other.
369
370 *3.5 Inter-clone group variability and summary*

When separating all single chamber Sr/Ca and Mg/Ca values into the three groups of clones, the resulting averages are very similar. Average Sr/Ca of all three groups is 1.56 mmol/mol, with variability (standard deviation) within groups of 0.11, 0.15 and 0.16 mmol/mol. Average Mg/Ca for the three groups is 3.68 mmol/mol (± 1.21, n=110), 3.51 mmol/mol (± 0.99, n=31) and 3.33 mmol/mol (± 0.80, n=32). Differences in single-chamber Sr/Ca and Mg/Ca between any combination of clone groups are not significant (two-tailed student's t-Test, assuming unequal variances, $p<0.95$), although the limited number of clone groups that are compared here hampers generalization of the calculated variability between them.

Average Mg/Ca and Sr/Ca and the variability of different hierarchical levels is summarized in Table 3.

Table 3: different levels of variability in Sr/Ca and Mg/Ca. The variability within test walls was determined on 12 individuals, displaying relatively high within-wall variability in Mg/Ca. The associated average standard deviation for these ablation profiles is ~40% of the average Mg/Ca. Calculated standard deviation for the inter-individual level is based on averages for the 22 individuals and the range in standard deviations for the clone groups represent the variability within these three groups.

4. Discussion

4.1 Reproduction, growth rates and size-normalized weights

Using the offspring of reproducing foraminifera provides a number of advantages for culturing studies. In a number of culture experiments growth is monitored by incorporation of a fluorescent marker (Bernhard et al., 2004) after which newly formed chambers (either stained or recognized after pre-incubation with the label) can be analyzed individually.

Although the effect of such markers on calcite Mg/Ca and Sr/Ca may be limited (Dissard et al., 2009), its complexation potential dictates the need to be accounted for in culturing studies (De Nooijer et al., 2007).

When culturing foraminifera with existing chambers, isotope- and element composition have to be corrected for the initial calcite weight of the test when whole individuals are analyzed (e.g. Kisakürek et al., 2011). Alternatively, newly formed chambers can be dissected from pre-existing chambers in planktonic species and pooled for analysis (e.g. Spero and Lea, 1996; Bijma et al., 1998). Using newborn clones (section 2.1; Hintz et al., 2006, McCorkle et al., 2008, Filipsson et al., 2010, Barras et al., 2010; Diz et al., 2012) circumvents the inaccuracies associated with such manipulations and allows analysis of the smallest foraminifer size fractions. Moreover, using LA-ICP-MS, the full range of chamber sizes can be analyzed for elements with sufficiently high concentrations (e.g. Reichart et al., 2003).

In our experiment, growth rates changed from approximately 1 chamber/day to 1 chamber/week. The time period between two chamber additions is relatively short in juveniles and increases as the individual matures (Figure 3A). Since mass increases exponentially with every chamber added in this species (Figure 3B), this results in a relatively constant rate of $CaCO_3$ addition over time (from approximately 0.70 to 0.15 µg/day for clone groups that grew slowest and fastest, respectively). The addition of calcite in foraminifera is however, concentrated into short time-intervals during which chambers are formed (~ hours; Keul et al., 2013).

Calcite precipitation rates are known to affect Sr/Ca, more than Mg/Ca (e.g. Lorens, 1981; Morse and Bender, 1990; Tesoriero and Pankow, 1996). A similar rate of calcite addition (in µg/ day) over time therefore fits the absence of an ontogenetic trend and limited variability of calcite Sr/Ca (and to a lesser extent Mg/Ca; Figures 5A and B, section 3.3). A caveat here is that overall calcite addition of an individual provides no information about crystal growth

421 rate, which is essentially unknown. Moreover, element partitioning in inorganically
422 precipitated calcites may not be directly comparable to that in foraminifera, since the
423 microenvironment in which foraminifera precipitate calcite is under biological control (e.g.
424 Erez, 2003; De Nooijer et al., 2009b) where element concentrations, pH, and the presence of
425 organic compounds can all differ from inorganic precipitation experiments.
426
427 *4.2. Test wall variability in Mg/Ca*
428 Magnesium is known to be heterogeneously distributed through chamber walls of a number of
429 species (Anand and Elderfield, 2005; Erez, 2003; Eggins et al., 2003; 2004; Hathorne et al.,
430 2003, 2009; Kunioka et al., 2006; Sadekov et al., 2005; 2008; Toyofuku and Kitazato, 2005;
431 Wit et al., 2010). Layers of calcite with high Mg/Ca observed within test walls are thought to
432 be the first calcite precipitated during a calcification event and are closely associated with the
433 primary organic sheet (Erez, 2003; Kunioka et al., 2006; Hathorne et al., 2009), although the
434 position of the primary, outer and inner organic linings (Hemleben et al., 1977) may correlate
435 with lowest Mg/Ca in other species (i.e. *Orbulina universa*; Eggins et al., 2004). In planktonic
436 foraminifera with photosynthetic symbionts, alternating bands of calcite with high and low
437 Mg/Ca ratios are thought to be a response to the diurnal light and dark cycle (Eggins et al.,
438 2004) although similar banding has been observed in non-spinose, symbiont-barren species
439 (Schmidt et al., 2008; Hathorne et al., 2009). Additionally, some studies have identified a
440 trace element enriched veneer with high Mg on foraminiferal tests (Eggins et al., 2003;
441 Hathorne et al., 2003, 2009; Sadekov et al., 2008).
442 The laser ablation profiles from our cultured individuals show a large variability in Mg/Ca
443 within a chamber wall and between chamber walls despite constant culturing conditions
444 (Figure 4). Early formed chambers that lie near the center of the individual contain relatively
445 more layers of calcite produced during consecutive chamber formation events. The absence of

446 an increase or decrease in Mg/Ca within these inner chambers fits with the absence of an
447 interchamber trend of Mg/Ca with size (Figure 5B). This is important to note, since the
448 lamellar structure of the ontogenetic calcite in ~~Rotallids~~ (Erez, 2003) may mask (subtle)
449 ontogenetic trends in chamber-to-chamber element distribution. The irregular position of the
450 Mg/Ca peaks in the profiles (Figure 4) furthermore suggests that the location of high-Mg
451 calcite is not related to the location of organic layers that separate the layers of lamellar
452 calcite (e.g. Hemleben et al., 1977).
453 Part of the variability in Mg- and Sr-incorporation observed in our dataset may be caused by
454 variability in the microenvironment between individuals. Respiration (e.g. Rink et al., 1998)
455 and proton pumping (Glas et al., 2012) during calcification alter the carbonate chemistry in
456 the direct surrounding of the test and thus may have an effect on the chemical speciation of
457 ions like Mg and Sr, thereby possibly affecting their uptake and eventually the calcite's Sr/Ca
458 and Mg/Ca. In *Ammonia*, ion pumping during calcification decreases the surrounding pH by
459 up to 1 unit (Glas et al., 2012). Since this decrease in pH is size-dependent, and the uptake of
460 Ca^{2+} (and possibly other cations like Mg and Sr too) takes place during calcification in
461 *Ammonia* (Nehrke et al., submitted), there may be a size-related change in Mg/Ca in our
462 cultured specimens. Since this is not the case (Figure 5 and accompanying text), it is unlikely
463 that pH in the foraminiferal microenvironment significantly impacts Mg/Ca. Since respiration
464 rates are likely to have a relatively small impact on ambient (pH) gradients, it is unlikely that
465 these processes can account for a large portion of the variability in Mg/Ca reported here.
466
467 *4.3 Interchamber and size-related variability in Sr/Ca and Mg/Ca*
468 In the *Ammonia tepida* samples from this study, there is no detectable control of coiling
469 direction or ontogeny (i.e. size-related) on Mg/Ca and Sr/Ca as the average ratios do not
470 change with size (number of chambers: Figure 5). This is in contrast with a number of reports

471 on size-specific Mg/Ca ratios in other species of benthic foraminifera from culturing
472 experiments (Hintz et al., 2006; Filipsson et al., 2010; Diz et al., 2012). Discrepancies
473 between studies could stem from species-specific differences in controls on element
474 incorporation, sample size, or both. Field studies of planktonic species show Mg/Ca increases
475 with size in some species and decreases with size in other species (Elderfield et al., 2002;
476 Anand and Elderfield, 2005; Friedrich et al., 2012), while under controlled constant
477 conditions, Mg/Ca of the planktonic *Globigerinoides sacculifer* decreases with size (Dueñas-
478 Bohórquez et al., 2011a). This implies that part of the relation between planktonic
479 foraminiferal shell size and Mg/Ca is determined by calcification at different water depths
480 (and hence different temperatures), and part of the ontogenetic controls on Mg/Ca are not
481 environment-induced. Raitzsch et al. (2011) show the variability of Mg/Ca and B/Ca ratios
482 are related within single tests of the benthic *Planulina wuellerstorfii* suggesting that changes
483 in carbonate chemistry within the sediment pore waters could be responsible for some of the
484 Mg/Ca variability. Interchamber variability may thus be explained by migration within the
485 sediment (for benthic species) or calcification at different ambient temperatures (for
486 planktonic species). Still, variability in Mg/Ca is often too large to be explained by vertical
487 migration (e.g. Hathorne et al., 2009).
488 Based on the interchamber variability of Mg/Ca in our dataset (Figure 5), we calculate that the
489 average Mg/Ca of the *A. tepida* populations can be estimated with a precision of 10% using 6
490 laser ablation measurements on different chambers (Figure 6). Under the controlled
491 conditions used here the number of individuals on which these 6 measurements are
492 performed, is irrelevant for the precision obtained. However, the interchamber (and
493 interindividual) variability in Mg/Ca may be different between species and depend on the
494 absolute Mg/Ca ratios. This means that the representativeness of 6 laser ablation
495 measurements may be better or worse for samples with other foraminiferal species.

496

497 *4.4 Interindividual and inter-clone group variability of Sr/Ca and Mg/Ca in* Ammonia *spp.*

498 A number of previous culturing experiments and field surveys using *Ammonia* spp. resulted
499 in similar Sr/Ca and Mg/Ca values ~~to~~ those presented here. In those studies calcitic Mg/Ca
500 was shown to depend on temperature (Toyofuku et al., 2011) and seawater [Ca^{2+}] (Raitzsch et
501 al., 2010). Studies of the dependence of calcitic Mg/Ca in benthic foraminifera on salinity
502 have produced contradictory results (Dissard et al., 2010a; Toyofuku et al., 2011; Diz et al.,
503 2012), while Mg/Ca in the calcite of cultured individuals of *Ammonia tepida* is not influenced
504 by seawater carbonate ion concentration (Dissard et al., 2010b; Dueñas-Bohórquez et al.,
505 2011b). Sr/Ca ratios of *A. tepida* are known to depend on seawater salinity (Dissard et al.,
506 2010a), whereas an effect of carbonate ion concentration is absent (Raitzsch et al., 2010;
507 Dueñas-Bohórquez et al., 2011b) or slightly positive (Dissard et al., 2010b).
508 Intra- and inter-individual variability in Mg/Ca is usually larger than that for Sr/Ca (e.g.
509 Allison and Austin, 2003). The large variability in Mg/Ca is attributed to a number of factors
510 including variability in environmental conditions (Wit et al., 2012), genetic differences
511 between individuals (Numberger et al., 2009), and ontogenetic effects (Elderfield et al.,
512 2002). Small fluctuations in experimental conditions cannot be responsible for the variability
513 in Mg/Ca, since the dependency of Mg/Ca on temperature and salinity is too small in
514 *Ammonia* spp to account for the observed variability (e.g. Toyofuku et al., 2011; this study).
515 Our results show that the small sample size afforded by LA-ICP-MS allows the detection of
516 interindividual (and intrachamber) variability in the Mg distribution. To account for this
517 small-scale variability, the average Mg/Ca of one or more complete individual tests can be
518 determined by combining multiple measurements on one individual (Figure 7).
519

520 *4.5 Implications for paleo-environmental studies*

521 The presence or absence of ontogenetic controls on element incorporation is important for the
522 use of foraminifera in paleoceanography. The recognition of size-related controls in Mg/Ca
523 (e.g. Dueñas-Bohórquez et al., 2011a) has lead to the proposal of using correction factors
524 when applying Mg/Ca-based temperature reconstructions. If the absence of an ontogenetic
525 trend (as observed here) is representative for foraminifera in general, ontogenetic trends found
526 in natural samples then most likely result from environmental changes (e.g. migration through
527 the water column for planktonic species). This changes the view of parts of the vital effect
528 from being 'biological noise' to being 'environmental information', the later potentially
529 providing a useful paleoclimate proxy.
530 Furthermore, our results show that despite substantial intra-test variability, the average Sr/Ca
531 of individual tests of *Ammonia tepida* is reproducible to ± 0.043 mmol/mol and Mg/Ca to 0.40
532 mmol/mol. These uncertainties are based on the variability between the average laser spot-
533 derived Sr/Ca and Mg/Ca when combining data from one individual (n=23; Figure 7).
534 Variability between single measurements is considerably larger (Figure 5). To translate the
535 Mg/Ca reproducibility into an error for temperature reconstructions using Mg/Ca data based
536 on single individuals, we have combined our results with those from previous culturing
537 studies (Figure 8). The *Ammonia* cultured by Dissard et al. (2010a; 2010b) and Dueñas-
538 Bohórquez et al. (2011b) were all collected from the Wadden Sea and cultured using similar
539 culturing set-ups. Together with our new data, these foraminifera were cultured at a range of
540 temperatures from 10 to 25 °C. The obtained exponential relationship between Mg/Ca and
541 temperature (R^2=0.86) is described by:
542
543 $Mg/Ca=0.167\ (\pm 0.064) * exp^{0.121\ (\pm 0.019)*T}$ (1)
544

According to the exponential factor, a change in Mg/Ca of 0.40 mmol/mol in *Ammonia tepida* (Figure 7) corresponds to a temperature change of 0.9 °C at 25 °C. It should be stressed that this uncertainty is based on the calculated inter-individual variability in Mg/Ca and at 25 °C only. The recently published Mg/Ca-T relationship of Toyofuku et al. (2011) produces a Mg/Ca for *Ammonia beccarii* at 25 °C (2 mmol/mol ± 0.3), approximately two times lower than that of *A. tepida* (equation 1). The exponential factor of the Mg/Ca-T relationship for *A. beccarii* is also approximately two times lower ($Mg/Ca=0.575*e^{0.0531*T}$) than found here. Mg/Ca from cultured *A. tepida* reported by Diz et al. (2012) fit the Mg/Ca-T calibration from Toyofuku et al. (2011) better than ~~that~~, presented here, suggesting that even within ~~one species~~, there may be (small) differences in the control on Mg-incorporation. Taxonomy for the genus *Ammonia* is notoriously unreliable (e.g. Holzmann et al., 2000; Hayward et al., 2004), and specimens commonly used for laboratory studies span a wide genetic range. Those employed by Toyofuku et al. (2011) are *Ammonia*'s of molecular type T4, those of Diz et al. (2012) of type T3 and those lumped for our calibration (Figure 8) are of molecular type T6 (Hayward et al., 2004), which may account for the variability in Mg/Ca-T calibrations reported so far. Differences in Mg/Ca ratios of the closely related ~~species~~, or even within one species underscores the need for species-specific calibrations before applying foraminiferal Mg/Ca in paleoceanographic reconstructions (e.g. Anand et al., 2003).

The error in a Mg/Ca-based reconstructed seawater temperature is a combination of the error arising from the inherent, biological variability in Mg/Ca (Figure 6) and that associated with the uncertainty in the Mg/Ca-T regression (equation 1). For a number of planktonic species, uncertainties in the Mg/Ca-temperature calibration are ~0.06 for the pre-exponential constant and ~0.02 for the exponential one (e.g. Dekens et al., 2002; Anand et al., 2003) and are similar to those reported here (equation 1). The uncertainty in the pre-exponential constant results in a temperature offset of 1.1 - 1.4 °C. Error propagation using partial derivatives of

570 this uncertainty and the one resulting from biological noise reported here (Figure 6), shows
571 that the total error in seawater temperature reconstruction is 2.1 °C at 25 °C and <1 °C at 10
572 °C, assuming a 5% error when using 20 laser ablation-derived Mg/Ca values. With only 6
573 laser ablation measurements (resulting in a ~10% error), the uncertainty in temperature
574 increases to 3.1 °C at 25 °C and 1.2 °C at 10 °C.
575
576 Figure 8: Mg/Ca-T relationship for cultured *A. tepida*. All culture data (Raitzsch et al., 2010;
577 Dissard et al., 2010a; 2010b; Dueñas-Bohórquez et al., 2011b; this study) are from individuals
578 grown at similar salinity (32-35) and inorganic carbon chemistry (e.g. pH 8.1-8.4 and [CO_3^{2-}]
579 of 160-260 μmol/kg). Symbols represent average Mg/Ca from all laser ablation data from
580 these studies.
581
582 The inherent, biological variability in Mg/Ca found here may be different at other
583 temperatures. If, however, the relative variability in Mg/Ca is similar (i.e. ~10%) across
584 temperatures, this would result in an error of ~0.75 °C at 1.0 °C and ~0.85 °C at 10 °C. If the
585 absolute variability in Mg/Ca (~0.40 mmol/mol) would be constant across temperatures,
586 absolute temperature estimates would be much more uncertain at lower temperatures.
587 Reported variability in Mg/Ca at different temperatures (e.g. Nürnberg et al., 1996; Sadekov
588 et al., 2008) seem to suggest that relative variability in Mg/Ca is similar across temperatures.
589
590 **Conclusions**
591 Our results show that Mg/Ca and Sr/Ca in the calcite of *Ammonia tepida* is not influenced by
592 ontogeny as there is no clear trend in the variability with size in the absence of environmental
593 change with ontogeny. The intra-chamber, inter-chamber and inter-individual variability of
594 Mg/Ca is larger than that of Sr/Ca, in line with previous studies of within shell element/Ca

595 ratios. Layers of calcite with elevated Mg/Ca within chamber walls appears to be responsible
596 for the variability in Mg/Ca. The presence of this higher Mg/Ca calcite is not related to
597 environmental conditions and is not correlated to genetic variability or similarity. With the
598 variability in calcitic Mg/Ca in our dataset, 6 laser ablation spots per individual *A. tepida* are
599 sufficient to estimate the average with an uncertainty of 10%, thereby accounting for the
600 biological noise on Mg/Ca-based temperature reconstructions.
601
602 **References**

603 Allison, N., Austin, W.E.N, 2003. The potential of ion microprobe analysis in detecting
604 geochemical variations across individual foraminifera tests. Geochem. Geophy. Geosy.
605 4, GC000430.
606 Anand, P., Elderfield, H., Conpte, M.H., 2003. Calibration of Mg/Ca thermometry in
607 planktonic foraminifera from a sediment trap time series. Paleoceanography 18,
608 PA000846.
609 Anand, P., Elderfield, H., 2005. Variability of Mg/Ca and Sr/Ca between and within the
610 planktonic foraminifers *Globigerina bulloides* and *Globorotalia truncatulinoides*.
611 Geochem. Geophy. Geosy. 6, Q11D15.
612 Barras, C., Duplessy, J.-C., Geslin, E., Michel, E., Jorissen, F.J., 2010. Calibration of $\delta^{18}O$ of
613 cultured benthic foraminiferal calcite as a function of temperature. Biogeosciences 7,
614 1349-1356.
615 Beer, C.J., Schiebel, R., Wilson, P.A., 2010. Testing planktonic foraminiferal shell weight as
616 a surface water [CO_3^{2-}] proxy using plankton net samples. Geology 38, 103-106.
617 Bemis, B.E., Spero, H.J., Lea, D.W., Bijma, J., 1998. Reevaluation of the oxygen isotopic
618 composition of planktonic foraminifera: Experimental results and revised
619 paleotemperature equations. Paleoceanography 13, 150-160.

620 Bentov, S., Erez, J., 2006. Impact of biomineralization processes on the Mg content of
621 foraminiferal shells: A biological perspective. Geochem. Geophy. Geosy. 7, GC001015.
622 Bernhard, J.M., Blanks, J.K., Hintz, C.J., Chandler, G.T., 2004. Use of fluorescent calcite
623 marker calcein to label foraminiferal tests. J. Foramin. Res. 34, 96-101.
624 Bijma, J., Hemleben, C., Huber, B.T., Erlenkeuser, H., Kroon, D., 1998. Experimental
625 determination of the ontogenetic stable isotope variability in two morphotypes of
626 *Globigerinella siphoniphera* (d'Orbigny). Mar. Micropaleontol. 35, 141-160.
627 Blackmon, P.D., Todd, R., 1959. Mineralogy of some foraminifera as related to their
628 classification and ecology. J. Paleontol. 33, 1–15.
629 Debenay, J.P., Bénéteau, E., Zhang, J., Stouff, V., Geslin, E., Redois, F., Fernandez-
630 Gonzalez, M., 1998. *Ammonia beccarii* and *Ammonia tepida* (Foraminifera):
631 morphofunctional arguments for their distinction. Mar. Micropaleontol. 34, 235-244.
632 Dekens, P.S., Lea, D.W., Pak, D.K., Spero, H.J., 2002. Core top calibration of Mg/Ca in
633 tropical foraminifera: Refining paleotemperature estimation. Geochem. Geophys.
634 Geosyst 3, 1022, doi: 10.1029/2001GC000200.
635 Delaney, M.L., Bé, A.W.H., Boyle, E.A., 1985. Li, Sr, Mg, and Na in foraminiferal calcite
636 shells from laboratory culture, sediment traps, and sediment cores. Geochim.
637 Cosmochim. Ac. 49, 1327-1341.
638 De Moel, H., Ganssen, G.M., Peeters, F.J.C., Jung, S.J.A., Kroon, D., Brummer, G.J.A.,
639 Zeebe, R.E., 2009. Planktic foraminiferal shell thinning in the Arabian Sea due to
640 anthropogenic ocean acidification? Biogeosciences 6, 1917-1925.
641 De Nooijer, L.J., Reichart, G.J., Dueñas-Bohórquez, A., Wolthers, M., Ernst, S.R., Mason,
642 P.R.D., Van der Zwaan G.J., 2007. Copper incorporation in foraminiferal calcite: results
643 from culturing experiments. Biogeosciences 4, 493-504.

644 De Nooijer, L.J., Toyofuku, T., Kitazato, H., 2009a. Foraminifera promote calcification by
645 elevating their intracellular pH. P. Natl. Acad. Sci. USA 106, 15374-15378.
646 De Nooijer, L.J., Langer, G., Nehrke, G., Bijma, J., 2009b. Physiological controls on the
647 seawater uptake and calcification in the benthic foraminifer *Ammonia tepida*.
648 Biogeosciences 6, 2669-2675.
649 Dissard, D., Nehrke, G., Reichart, G.J., Bijma, J., 2009. Effect of the fluorescent indicator
650 calcein on Mg and Sr incorporation in foraminiferal calcite. Geochem. Geophy. Geosy.
651 10, Q11001.
652 Dissard, D., Nehrke, G., Reichart, G.J., Bijma, J., 2010a. The impact of salinity on the Mg/Ca
653 and Sr/Ca ratio in the benthic foraminifera *Ammonia tepida*: Results from culture
654 experiments. Geochim. Cosmochim. Ac. 74, 928–940.
655 Dissard, D., Nehrke, G., Reichart, G.J., Bijma, J., 2010b. Impact of seawater pCO_2 on
656 calcification and Mg/Ca and Sr/Ca ratios in benthic foraminifera calcite: results from
657 culturing experiments with *Ammonia tepida*. Biogeosciences 7, 81-93.
658 Diz, P., Jorissen, F.J., Reichart, G.J., Poulain, C., Dehairs, F., Leorri, E., Paulet, Y.-M., 2012.
659 Interpretation of benthic foraminiferal stable isotopes in subtidal estuarine
660 environments. Biogeosciences 6, 2549-2560.
661 Dueñas-Bohórquez, A., Da Rocha, R.E., Kuroyanagi, A., Bijma, J., Reichart, G.J., 2009.
662 effect of salinity and seawater calcite saturation state on Mg and Sr incorporation in
663 cultured planktonic foraminifera. Mar. Micropaleontol. 73, 178-189.
664 Dueñas-Bohórquez, A., Da Rocha, R.E., Kuroyanagi, A., De Nooijer, L.J., Bijma, J.,
665 Reichart, G.J., 2011a. Interindividual variability and ontogenetic effects on Mg and Sr
666 incorporation in the planktonic foraminifer *Globigerinoides sacculifer*. Geochim.
667 Cosmochim. Ac. *75*, 520-532.

668 Dueñas-Bohórquez, A., Raitzsch, M., De Nooijer, L.J., Reichart, G.J., 2011b. Independent
669 impacts of calcium and carbonate ion concentration on Mg and Sr incorporation in
670 cultured benthic foraminifera. Mar. Micropaleontol. 81, 122-130.
671 Eggins, S.M., De Deckker, P., Marshall, J., 2003. Mg/Ca variation in planktonic foraminifera
672 tests: implications for reconstructing palaeo-seawater temperature and habitat migration.
673 Earth Planet. Sc. Lett. 212, 291-306.
674 Eggins, S.M., Sadekov, A., De Deckker, P., 2004. Modulation and daily banding of Mg/Ca in
675 *Orbulina universa* tests by symbiont photosynthesis and respiration: a complication for
676 sea water thermometry? Earth Planet. Sc. Lett. 225, 411-419.
677 Elderfield, H., Ganssen, G.M., 2000. Past temperature and $\delta^{18}O$ of surface ocean waters
678 inferred from foraminiferal Mg/Ca ratios. Nature 405, 442-445.
679 Elderfield, H., Vautravers, M., Cooper, M., 2002. The relationship between shell size and
680 Mg/Ca, Sr/Ca, $\delta^{18}O$, and $\delta^{13}C$ of species of planktonic foraminifera. Geochem.,
681 Geophy., Geosy. 3, 10.1029/2001GC000194.
682 Erez, J., 2003. The source of ions for biomineralization in foraminifera and their implications
683 for paleoceanographic proxies. in Reviews in Mineralogy and Geochemistry, vol. 54,
684 edited by Dove, P.M., and De Yoreo, J.J., pp. 115-149, Mineralogical Society of
685 America, Geochemical Society.
686 Filipsson, H., Bernhard, J.M., Lincoln, S.A., McCorkle, D.C., 2010. A culture-based
687 calibration of benthic foraminiferal paleotemperature proxies: $\delta^{18}O$ and Mg/Ca results.
688 Biogeosciences 7, 1335-1347.
689 Friedrich, O., Schiebel, R., Wilson, P.A., Weldeab, S., Beer, C.J., Cooper, M.J., Fiebig, J.,
690 2012. Influence of test size, water depth, and ecology on Mg/Ca, Sr/Ca, delta-O18 and
691 delta-C13 in nine modern species of planktonic foraminifera, Earth Planet. Sci. Lett.
692 319, 133-145.

693 Ganssen, G.M., Peeters, F.J.C., Metcalfe, B., Anand, P., Jung, S.J.A., Kroon, D., Brummer,
694 G.J.A., 2011. Quantifying sea surface temperature ranges of the Arabian Sea for the past
695 20,000 years. Clim. Past 7, 1337-1349.
696 Glas, M., Langer, G., Keul, N., 2012. Calcification acidifies the microenvironment of a
697 benthic foraminifer (*Ammonia* sp.). J. Exp. Mar. Biol. Ecol. 424-425, 53-58.
698 Goldstein, S.T., Moodley, L.M., 1993. Gametogenesis and the life cycle of the foraminifer
699 *Ammonia beccarii* (Linné) forma tepida (Cushman). J. Foraminif. Res. 23, 213-220.
700 Haarmann, T., Hathorne, E.C., Mohtadi, M., Groeneveld, J., Kölling, M., Bickert., T., 2011.
701 Mg/Ca ratios of single planktonic foraminifer shells and the potential to reconstruct the
702 thermal seasonality of the water column. Paleoceanography 26, PA3218.
703 Hathorne, E.C., Alard, O., James, R.H., Rogers, N.W., 2003. Determination of intratest
704 variability of trace elements in foraminifera by laser ablation inductively coupled mass
705 spectrometry. Geochem. Geophy. Geosy. 4, GC000539.
706 Hathorne, E.C., James, R.H., Savage, P., Alard., O., 2008. Physical and chemical
707 characteristics of particles produced by laser ablation of biogenic calcium carbonate. J.
708 Anal. Atom. Spectrom. 23, 240-243.
709 Hathorne, E.C., James, R.H., Lampitt, R.S., 2009. Environmental versus biomineralization
710 controls on the intratest variation in the trace element composition of the planktonic
711 foraminifera *G. inflata* and *G. scitula*. Paleoceanography 24, PA4204.
712 Hayward, B.W., Holzmann, M., Grenfell, H.R., Pawlowski, J., Triggs, C.M., 2004.
713 Morphological distinction of molecular types in *Ammonia* – towards a taxonomic
714 revision of the world's most commonly misidentified foraminifera. Mar.
715 Micropaleontol. 50, 237-271.

716 Hemleben, C., Bé, A.W.H., Anderson, O.R., Tuntivate, S., 1977. Test morphology, organic
717 layers and chamber formation of the planktonic foraminifer *Globorotalia menardii*
718 (D'Orbigny). J. Foram. Res. 7, 1-25.
719 Hintz, C.J., Shaw, T.J., Chandler, G.T., Bernhard, J.M., McCorkle, D.C., Blanks, J.K., 2006.
720 Trace/ minor element: calcium ratios in cultured benthic foraminifera. Part II:
721 Ontogenetic variation. Geochim. Cosmochim. Ac. 70, 1964-1976.
722 Ho, T.Y., Quigg, A., Finkel, Z.V., Milligan, A.J., Wyman, K., Falkowski, P.G., Morel,
723 F.M.M., 2003. The elemental composition of some marine phytoplankton. J. Phycol. 39,
724 1145-1159.
725 Holzmann, M., Pawlowski, J., 1997. Molecular, morphological and ecological evidence for
726 species recognition in *Ammonia* (Foraminifera). J. Foraminif. Res. 27, 311-318.
727 Holzmann, M., Pawlowski, J., 2000. Taxonomic relationships in the genus *Ammonia*
728 (Foraminifera) based on ribosomal DNA sequences. J. Micropaleont. 19, 85-95.
729 Inoue, M., Nohara, M., Okai, T., Suzuki, A., Kawahata, H., 2004. Concentrations of trace
730 elements in carbonate reference materials coral JCp-1 and giant clam JCt-1 by
731 inductively coupled plasma-mass spectrometry. Geostand. Geoanal. Res. 28, 411-416.
732 Jochum, K.P., Weis, U., Stoll, B., Kuzmin, D., Yang, Q., Raczek, I., Jacob, D.E., Stracke, A.,
733 Birbaum, K., Frick, D.A., Günther, D., Enzweiler, J., 2011. Determination of reference
734 values for NIST SRM 610-617 glasses following ISO guidelines. Geostand. Geoanal.
735 Res. 35, 397-429.
736 Keul, N., Langer, G., De Nooijer, L.J., Bijma, J., 2013. Effect of ocean acidification on the
737 benthic foraminifera *Ammonia* sp. is caused by a decrease in carbonate ion
738 concentration. Biogeosciences Discuss. 10, 1147-1176.

739 Khider, D., Stott, L.D., Emile-Gray, J., Thunell, R., Hammond, D.E., 2011. Assessing El
740 Niño southern oscillation variability during the past millennium. Paleoceanography 26,
741 PA3222.
742 Kisakürek, B., Eisenhauer, A., Böhm, F., Hathorne, E.C., Erez, J., 2011. Controls on calcium
743 isotope fractionation in cultured planktonic foraminifera, *Globigerinoides ruber* and
744 *Globigerinella siphonifera*. Geochim. Cosmochim. Ac. 75, 427-443.
745 Kunioka, D., Shirai, K., Takahata, N., Sano, Y., Toyofuku, T., Ujiie, Y., 2006.
746 Microdistribution of Mg/Ca, Sr/Ca, and Ba/Ca ratios in *Pulleniantina obliquilloculata*
747 test by using a NanoSIMS: Implication for the vital effect mechanism. Geochem.
748 Geophy. Geosy. 7, Q12P20.
749 Lear, C.H., Elderfield, H., Wilson, P.A., 2000. Cenozoic deep-sea temperatures and global ice
750 volumes from Mg/Ca ratios in benthic foraminiferal calcite. Science 287, 269-272.
751 Lorens, R.B., 1981. Sr, Cs, Mn and Co distribution coefficients in calcite as a function of
752 calcite precipitation rate. Geochim. Cosmochim. Ac. 45, 553-561.
753 Morse, J.W., Bender, M.L., 1990. Partition coefficients in calcite: Examination of factors
754 influencing the validity of experimental results and their application to natural systems.
755 Chem. Geol. 82, 265-277.
756 Mortyn, P.G., Elderfield, H., Anand, P., Greaves, M., 2005. An evaluation of controls on
757 planktonic foraminiferal Sr/Ca: Comparison of water column and core-top data from a
758 North Atlantic transect. Geochem. Geophy. Geosy. 6, Q12007.
759 Mucci, A., 1987. Influence of temperature on the composition of magnesian calcite
760 overgrowths precipitated from seawater. Geochim. Cosmochim. Ac. 51, 1977-1984.
761 Numberger, L., Hemleben, C., Hoffmann, R., Mackensen, A., Schultz, H., Wunderlich, J.-M.,
762 Kucera., M., 2009. Habitats, abundance patterns and isotopic signals of morphotypes of
763 the planktonic foraminfer *Globigerinoides ruber* (d'Orbigny) in the eastern

764 Mediterranean Sea since the Marine Isotopic Stage 12. Marine Micropaleontology 73,
765 90-104.
766 Nürnberg, D., Bijma, J., Hemleben, C., 1996. Assessing the reliability of magnesium in
767 foraminiferal calcite as a proxy for water mass temperatures. Geochim. Cosmochim.
768 Ac. 60, 803-814.
769 Okai, T., Suzuki, A., Kawahata, H., Terashima, S., Imai, N., 2002. Preparation of a new
770 Geological Survey of Japan geochemical reference material: coral JCp-1. Geostandards
771 Newsletter 26, 95-99.
772 Okai, T., Suzuki, A., Terashima, S., Inoue, M., Nohara, M., Kawahata, H., Imai., N., 2004.
773 Collaborative analysis of GSJ/AIST geochemical reference materials JCp-1 (Coral) and
774 JCt-1 (Giant Clam). Chikyukagaku (Geochemistry), 38, 281-286.
775 Oomori, T., Kaneshima, H., Maezato, Y., 1987. Distribution coefficient of Mg^{2+} ions between
776 calcite and solution at 10-50°C. Mar. Chem. 20, 327-336.
777 Raitzsch, M., Dueñas-Bohorquez, A., Reichart, G.J., De Nooijer, L.J., Bijma, J., 2010.
778 Incorporation of Mg and Sr in calcite of cultured benthic foraminifera: impact of
779 calcium concentration and associated calcite saturation state. Biogeosciences 7, 869-
780 881.
781 Raitzsch, M., Hathorne, E.C., Kuhnert, H., Groeneveld, J., Bickert, T., 2011a. Modern and
782 Late Pleistocene B/Ca ratios of the benthic foraminifer *Planulina wuellerstorfi*
783 determined with laser ablation ICP-MS. Geology 39, 1039-1042.
784 Raitzsch, M., Kuhnert, H., Hathorne, E.C., Groeneveld, J., Bickert, T., 2011b. U/Ca in benthic
785 foraminifers: A proxy for the deep-sea carbonate saturation. Geochem. Geophy. Geosy.
786 12, Q06019.

787 Rathburn, A.E., De Deckker, P., 1997. Magnesium and strontium compositions of recent
788 benthic foraminifera from the Coral Sea, Australia and Prydz Bay, Antarctica. Mar.
789 Micropaleontol. 32, 231-248.
790 Reichart, G.J., Jorissen, F.J., Anschutz, P., Mason, P.R.D., 2003. Single foraminiferal test
791 chemistry records the marine environment. Geology 31, 355-358.
792 Reiss, Z., 1957. The Bilamellidae, nov. superfam. and remarks on Cretaceaous Globorotaliids.
793 Contrib. Cushman Found. Foram. Res. 8, 127-145.
794 Rimstidt, J.D., Balog, A., Webb, J., 1998. Distributions of trace elements between carbonate
795 minerals and aqueous solutions. Geochim. Cosmochim. Ac. 62, 1851-863.
796 Rink, S., Kühl, M., Bijma, J., Spero, H.J., 1998. Microsensor studies of photosynthesis and
797 respiration in the symbiotic foraminifer *Orbulina universa*. Mar. Biol. 131, 583-595.
798 Rosenthal, Y., Boyle, E.A., Slowley, N., 1997. Temperature control on the incorporation of
799 magnesium, strontium, fluorine, and cadmium into benthic foraminiferal shells from
800 Little Bahama Bank: prospects for thermocline paleoceanography. Geochim.
801 Cosmochim. Ac. 61, 3633-3643.
802 Rosenthal, Y., Lear, C.H., Oppo, D.W., Linsley, B.K., 2006. Temperature and carbonate ion
803 effects on Mg/Ca and Sr/Ca ratios in benthic foraminifera: Aragonitic species
804 *Hoeglundina elegans*. Paleoceanography 21, PA1007.
805 Sadekov, A.Y., Eggins, S.M., De Deckker, P., 2005. Characterization of Mg/Ca distributions
806 in planktonic foraminifera species by electron microprobe mapping. Geochem. Geophy.
807 Geosy. 6, Q12P06.
808 Sadekov, A.Y., Eggins, S.M., De Deckker, P., Kroon, D., 2008. Uncertainties in seawater
809 thermometry deriving from intratest and intertest Mg/Ca variability in *Globigerinoides*
810 *ruber*. Paleoceanography 23, PA1215.
811 Schmidt, D.N., Elliot,T., Kasemann, S.A., 2008. The influences of growth rates on planktic
812 foraminifers as proxies for paleostudies - a review, in *Biogeochemical controls on*

palaeoceanographic environmental proxies, vol. 303, edited by Austin, W.E.N., James R.H., pp. 73-85, Geological Society, London, Special Publications.

Schmiedl, G., Pfeilsticker, M., Hemleben, C., Mackensen, A., 2004. Environmental and biological effects on the stable isotope composition of recent deep-sea benthic foraminifera from the western Mediterranean Sea. Mar. Micropaleontol. 51, 129-152.

Spero, H.J., Lea, D.W., 1996. Experimental determination of stable isotope variability in *Globigerina bulloides*: implications for paleocanographic reconstructions. Mar. Micropaleontol. 28, 231-246.

Stouff, V., Lesourd, M., Debenay, J.P., 1999. Laboratory observations on asexual reproduction (schizogony) and ontogeny of *Ammonia tepida* with comment on the life cycle. J. Foraminif. Res. 29, 75-84.

Tesoriero, A.J., Pankow, J.F., 1996. Solid solution partitioning of Sr^{2+}, Ba^{2+}, and Cd^{2+} to calcite. Geochim. Cosmochim. Ac. 60, 1053-1063.

Toyofuku, T., Kitazato, H., 2005. Micromapping of Mg/Ca values in cultured specimens of the high magnesium benthic foraminifera. Geochem. Geophy. Geosy. 6, GC000961.

Toyofuku, T., Suzuki, M., Suga, H., Sakai, S., Suzuki, A., Ishikawa, T., De Nooijer, L.J., Schiebel, R., Kawahata, H., Kitazato, H., 2011. Mg/Ca and $\delta^{18}O$ in the brackish shallow-water benthic foraminifer *Ammonia beccarii*. Mar. Micropaleontol. 78, 113-120.

Van Aken, H.M., 2008. Variability of the water temperature in the Western Wadden Sea on tidal to centennial time scales. J. Sea Res. 60, 227-234.

Wefer, G., Killingley, J.S. Lutze, G.F., 1981. Stable isotopes in recent larger foraminifera. Palaeogeogr. Palaeocl. Palaeoecol. 33, 253-270.

836 Wit, J.C., Reichart, G.J., Jung, S.J.A., Kroon, D., 2010. Approaches to unravel seasonality in
837 sea surface temperatures using paired single-specimen foraminiferal $\delta^{18}O$ and Mg/Ca
838 analyses. Paleoceanography 25, PA4220.
839 Wit, J.C., De Nooijer, L.J., Barras, C., Jorissen, F.J., Reichart, G.J., 2012. A reappraisal of the
840 vital effect in cultured benthic foraminifer *Bulimina marginata* on Mg/Ca values:
841 assessing temperature uncertainty relationships. Biogeosciences 9, 3693-3704.

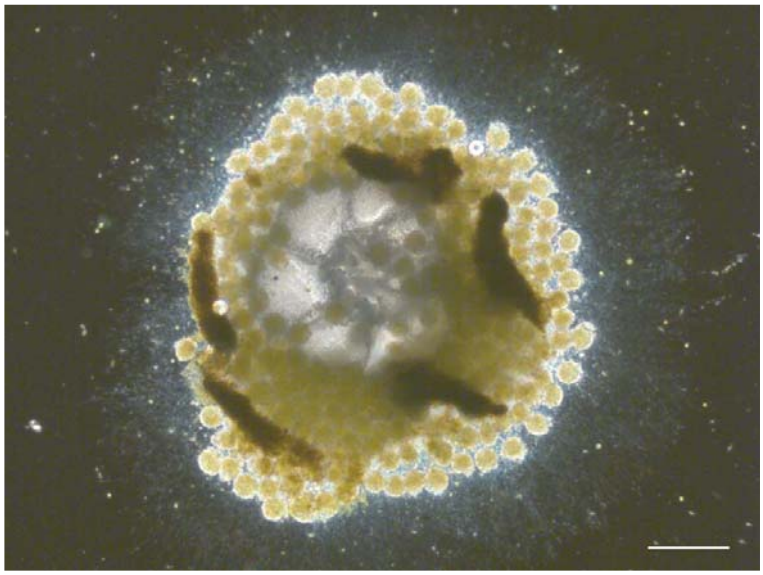

Figure 1: Asexual reproduction in *Ammonia tepida*. The empty test of the adult (i.e. 'parent') individual is surrounded by approximately 200 juveniles that have emerged from the aperture. The single-chambered juveniles form a relatively large and dense pseudopodial network that they use to move away from the parent in the following hours. The dark masses are remains of the food cyst that surrounded the adult foraminifer before reproduction. Scale bar = 100µm.

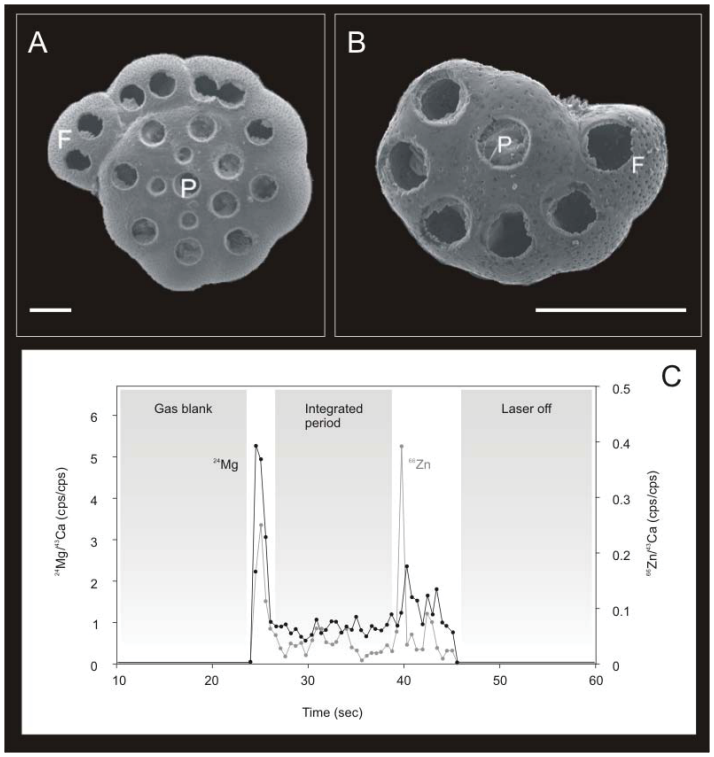

Figure 2: Example of two individuals (A and B) after LA-ICP-MS. P=proloculus, F=final chamber. Scale bar = 100µm. C: example of a laser ablation profile with high Mg/Ca and Zn/Ca indicative of residual cytoplasm on both sides of the chamber wall.

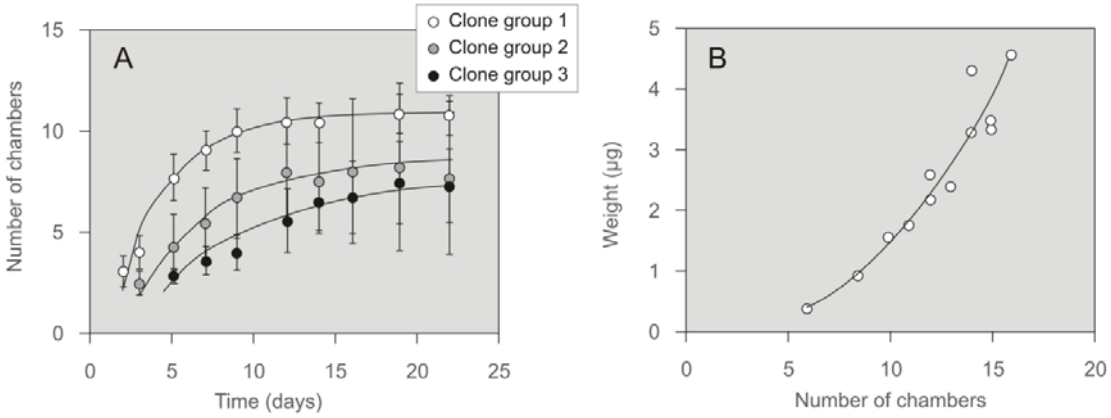

Figure 3: Growth rates (A, ± 1 standard deviation) for each of the three clone groups and chamber-normalized weights (B) of cultured *A. tepida*. The weight of tests increases exponentially with every chamber being added (R^2=0.934; compared to 0.888 for a linear fit) and is described by: $w=0.138e^{0.225n}$, where w is the $CaCO_3$ weight of an individual test in µg and n is the chamber number (1= proloculus).

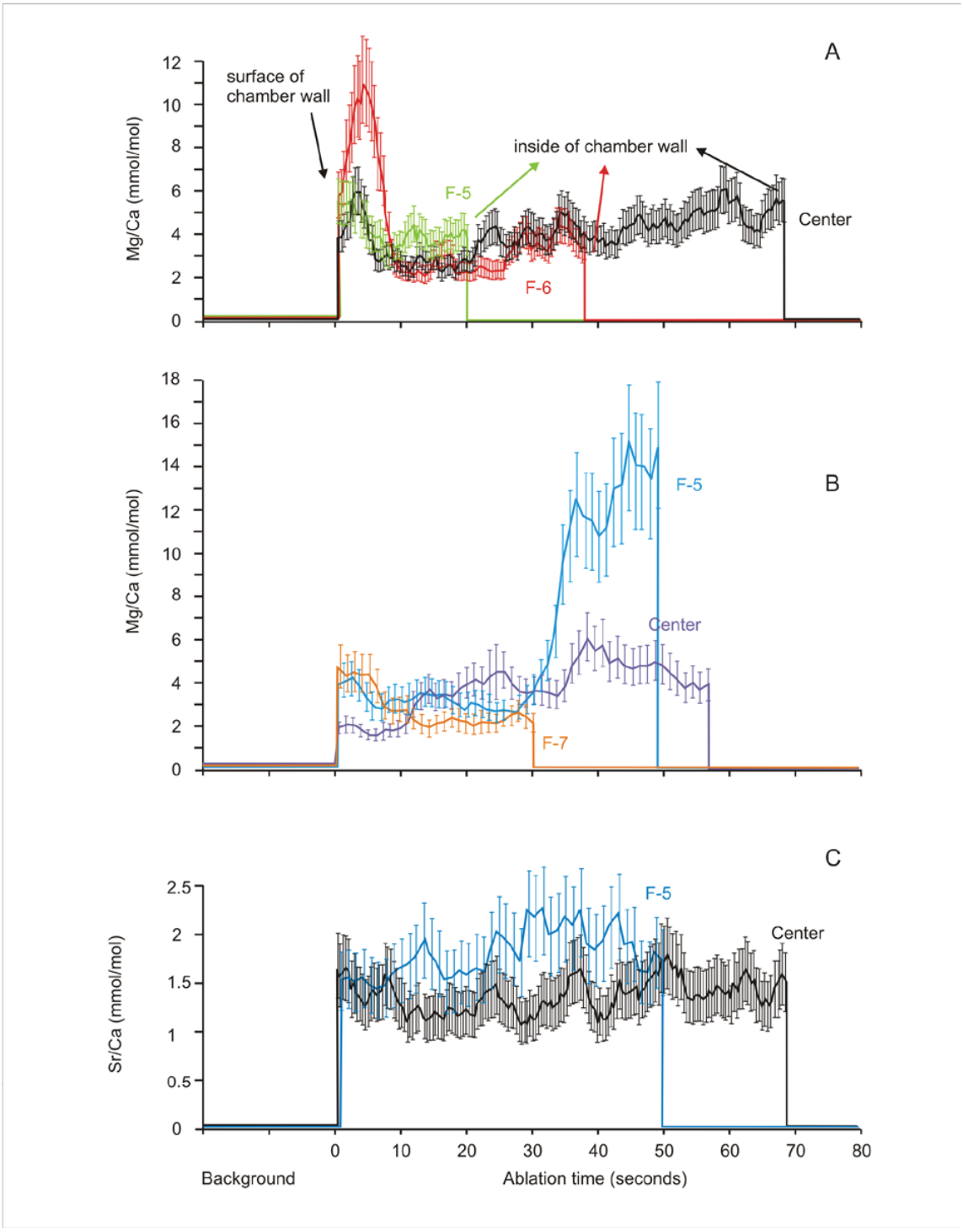

Figure 4: Sr/Ca and Mg/Ca ablation profiles from cultured *Ammonia tepida*. A: Sr/Ca of one chambers obtained at Utrecht University (in black) and one obtained at GEOMAR (in blue), B: Mg/Ca of three different chambers obtained at Utrecht University, C: Mg/Ca of three different chambers obtained at GEOMAR. Error bars are based on within-profile variability of a powder pellet of the JCp-1 carbonate standard (Okai et al., 2002; 2004).

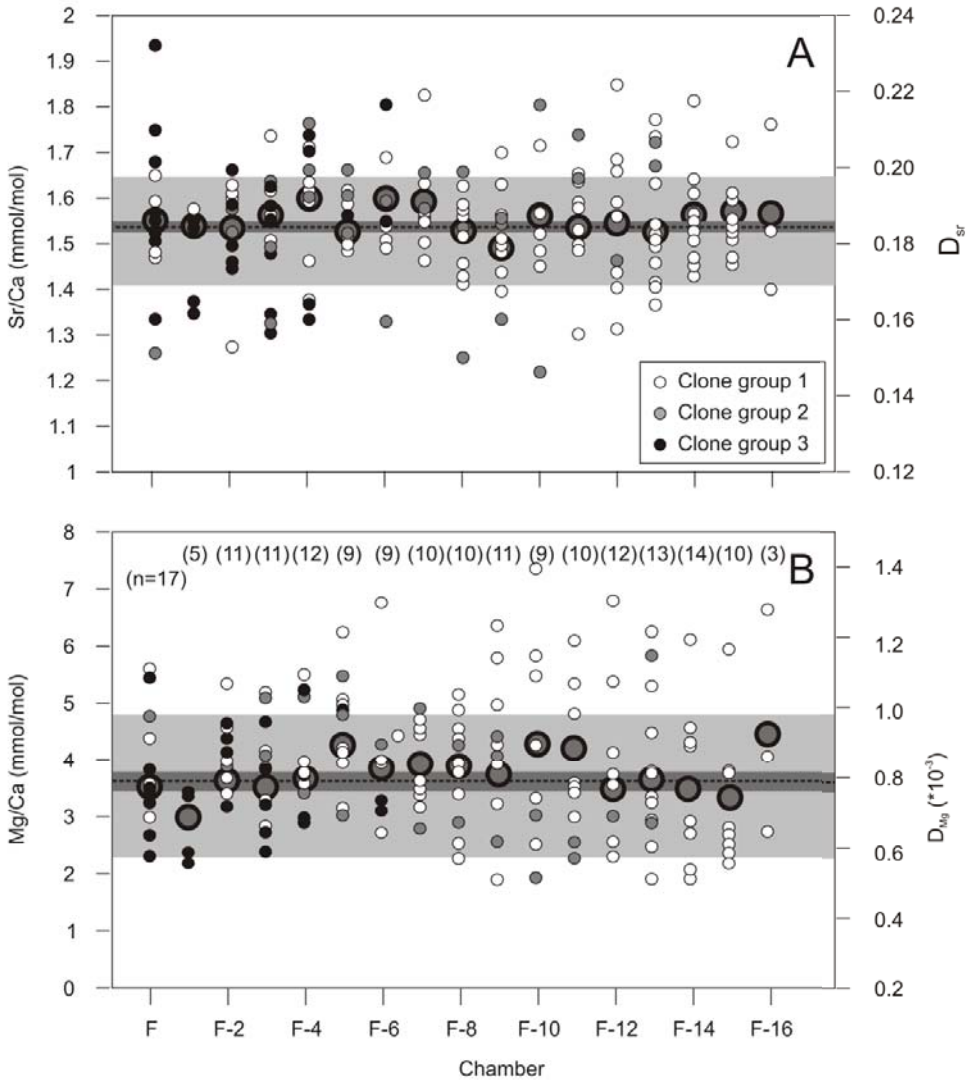

Figure 5: Average Sr/Ca (panel A), Mg/Ca (panel B) and partition coefficients (D_{Sr} and D_{Mg}) from single-chamber analyses of 30 individuals of cultured *A. tepida* as a function of the position within the foraminifer. Every point represents one laser ablation spot. On the left side, analyses of the final (F) chamber are plotted, while measurements towards the right side represent Sr/Ca and Mg/Ca from older chambers. Black, grey and white symbols represent the three different clone groups. Larger circles represent average Sr/Ca and Mg/Ca for each chamber position. The dotted line and surrounding grey box represent the average ± 1 standard error of the mean. The lighter grey box represents ± 1 standard deviation. Number of laser ablation spots per chamber position is indicated in at the upper side of panel B.

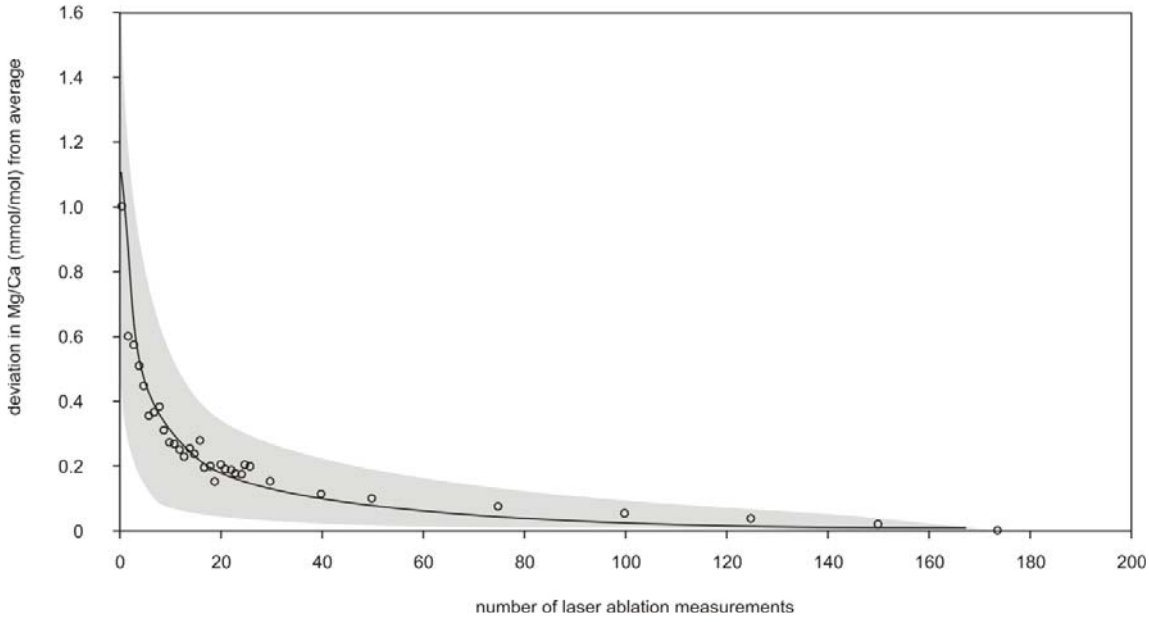

Figure 6: relation between number of laser ablation spots and deviation from the set average Mg/Ca (n=50, see text for explanation) from the average Mg/Ca of the complete dataset (=3.6 mmol/mol). With ~6 laser ablation measurements on different chambers (or positions on the test) the deviation is approximately 10% of the average of the dataset, with ~20 measurements, the estimated Mg/Ca is within 5% of the average of the complete dataset.

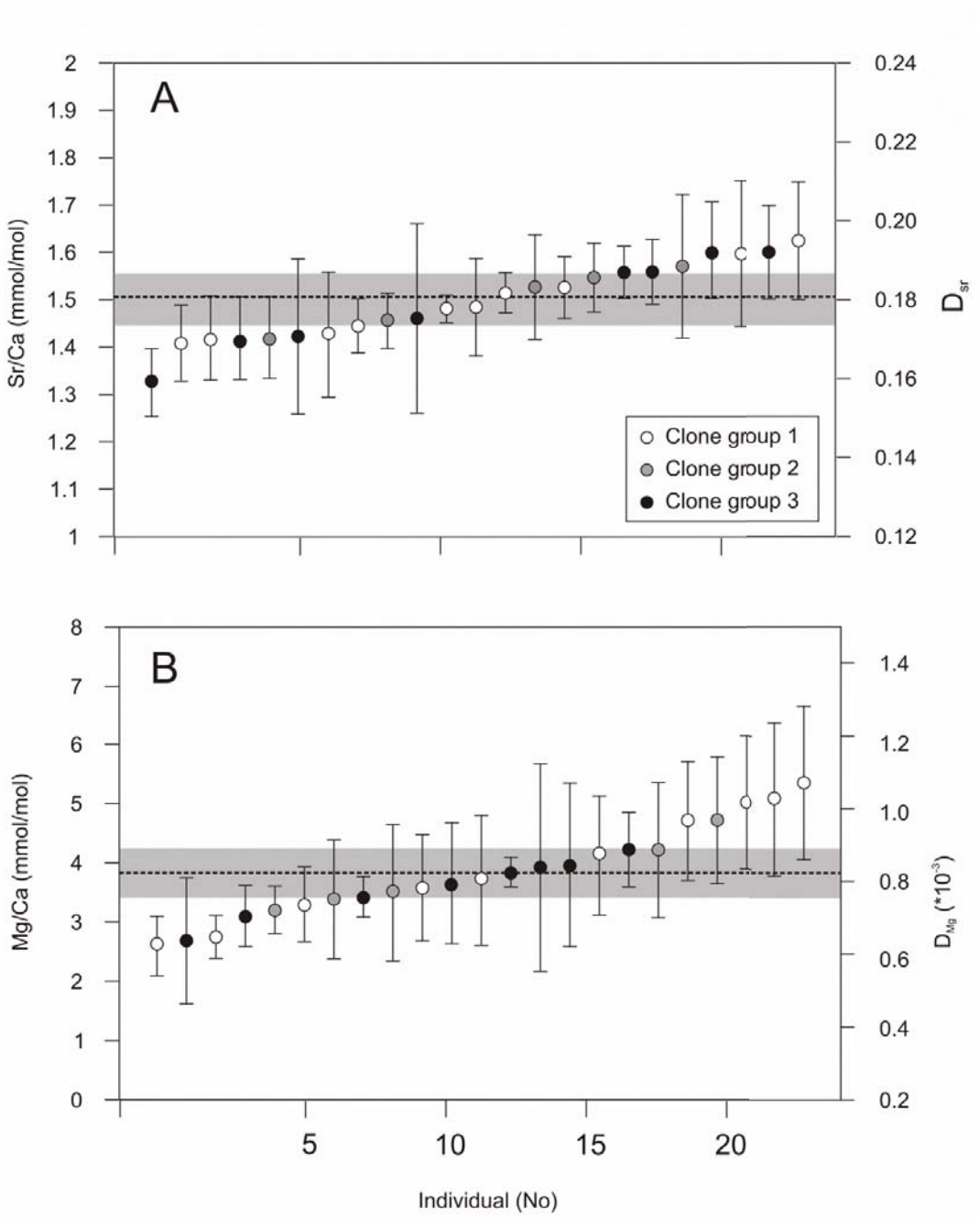

Figure 7: A: Variability of single individual Sr/Ca in cultured *A. tepida*. Results from all laser spots (Figure 5A) are combined to display the inter-individual variability in Sr/Ca (average per individual ± 1 standard deviation). These data have been ranked according to their Sr/Ca ratio for clarity but note that the ranking for inter-individual Mg/Ca is different. B: Variability of Mg/Ca in cultured individuals. Results from single-chamber measurements (Figure 5B) are combined to display the inter-individual variability in Mg/Ca (average per individual ± 1 standard deviation). For both panels, dotted horizontal line is the average element/Ca of all individuals and accompanying dark grey box represents 1 standard deviation.

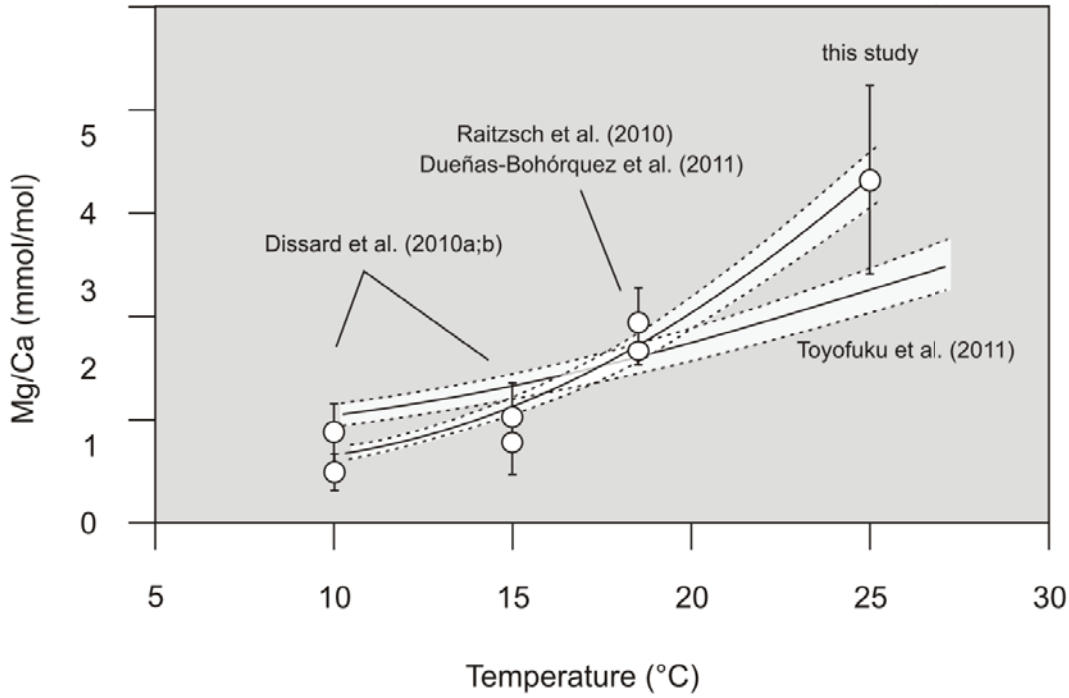

Figure 8: Mg/Ca-T relationship for cultured *A. tepida*. All culture data (Raitzsch et al., 2010; Dissard et al., 2010a; 2010b; Dueñas-Bohórquez et al., 2011b; this study) are from individuals grown at similar salinity (32-35) and inorganic carbon chemistry (e.g. pH 8.1-8.4 and $[CO_3^{2-}]$ of 160-260 µmol/kg). Symbols represent average Mg/Ca from all laser ablation data from these studies.

Table 1: Settings and details of the different laser systems employed in this study.

Laboratory	Bremen	Utrecht	Kiel
Manufacturer	NWR	Geolas 200Q	NWR
Laser	193 nm solid state	193 nm Excimer	193 nm Excimer
Energy density	~0.35 GW/cm^2	~1 J/cm^2	~1 J/cm^2
Laser spot size	35/ 75 µm	40 µm	25/ 50 µm
Ablation frequency	5 Hz	7 Hz	4/ 5 Hz
Results	Figure 5 and 7	Figure 4A, B	Figure 4B, C

Table 2: Reproduction, growth and amount of calcite available for chemical analyses. Dextral coiling is clockwise addition of chambers on the spiral side: sinistral is anti-clockwise. 'n.d.'= not determined.

	Clone Group 1	Clone Group 2	Clone Group 3
Number of juveniles	244	116	103
Incubation time (days)	21	17	17
Chambers after incubation	14.7 ± 2.0 (n=94)	12.2 ± 2.1 (n=96)	5-7 (n=50)
Mean growth rate (chambers added/ day)	0.70	0.72	0.35
Dextral coiling	52% (n=94)	35% (n=55)	n.d.
Sinistral coiling	48% (n=94)	65% (n=55)	n.d.
Individuals analyzed for element/Ca	10	5	10
Chambers analyzed for element/Ca	111	42	32

Table 3: different levels of variability in Sr/Ca and Mg/Ca. The variability within test walls was determined on 12 individuals, displaying relatively high within-wall variability in Mg/Ca. The associated average standard deviation for these ablation profiles is ~40% of the average Mg/Ca. Calculated standard deviation for the inter-individual level is based on averages for the 22 individuals and the range in standard deviations for the clone groups represent the variability within these three groups.

	Sr/Ca		Mg/Ca	
	Range (min-max in mmol/mol)	SD	Range (min-max in mmol/mol)	SD
Within test walls (n=12)	1.0 - 2.5	0.39/ ablation profile	1.1 - 14	1.9/ ablation profile
Inter-chamber (n=173)	1.2 - 2.0	0.13	1.7 - 7.0	1.2
Inter-individual (n=22)	1.4 - 1.7	0.084	2.5 - 5.0	0.72
Within clone group (n=3)	1.56	0.11 - 0.16	3.33 - 3.68	0.80 - 1.2